Carbohydrate Research, 29 (1973) 123–134

INFRARED AND RAMAN SPECTROSCOPY OF CARBOHYDRATES

PART III: RAMAN SPECTRA OF THE POLYMORPHIC FORMS OF AMYLOSE

J. J. CAEL, J. L. KOENIG, AND J. BLACKWELL

Division of Macromolecular Science, Case Western Reserve University, Cleveland, Ohio 44106 (U. S. A.)

(Received September 22nd, 1972; accepted with revisions November 20th, 1972)

ABSTRACT

The Raman spectra of V_a-, V_h-, and B-amylose have been recorded, and are interpreted in terms of the proposed mechanism for conversion from the V- into the B-form. Lines occurring at 1263 and 946 cm^{-1} with V-amylose shift to 1254 and 936 cm^{-1} on conversion into the B-form; at the same time intensity changes are observed for the lines at 2940 and 1334 cm^{-1}. These effects are consistent with the mechanism proposed for V→B conversion, involving an extension of the helix and changes in the intramolecular hydrogen-bonding. In addition, the spectra of amylose dissolved in aqueous salt solution and in methyl sulfoxide have been recorded. The results indicate that amylose does not adopt the V-conformation in methyl sulfoxide solution.

INTRODUCTION

Amylose and amylopectin serve as food-storage carbohydrates in plants, where they occur in starch granules. Both of these polysaccharides are made up of α-(1→4)-linked D-glucose residues; amylose is the linear polymer (Fig 1), whereas amylopectin has some α-(1→6) branching. Starch is considered to occur in three crystalline forms, differentiated by their X-ray diffraction patterns[1]. The A-form is found in cereal starch, whereas the B-form occurs in tuber starches; the C-form is more rare and has been observed in, for example, tapioca and banana starches. All three X-ray patterns can also be obtained with isolated amylose, and the X-ray patterns of starch are probably due to the amylose component and oriented, straight-chain sections of amylopectin. It seems that the A-, B-, and C-structures are very similar, and are probably different hydrates having the same chain conformation[2].

Amylose can be isolated from starch by precipitation from solution with various organic solvents such as butyl alcohol. The precipitated amylose is generally complexed with solvent molecules and exhibits the X-ray pattern of the so called V-form. Removal of the complexing agent by using aqueous methanol yields the V_a-structure; the suffix was originally used to indicate what was thought to be an anhydrous structure, but this form almost certainly contains some water molecules within the crystal lattice. The V_a-structure has been shown by X-ray diffraction[3,4] to consist of

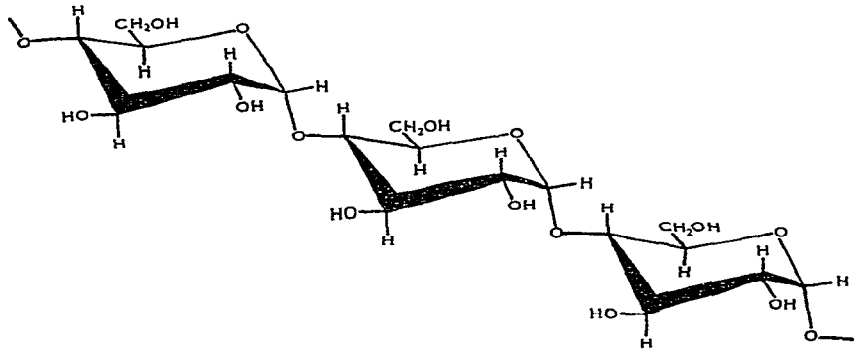

Fig. 1. Structural formula for amylose.

amylose helices having six glucose residues per turn, repeating in 7.90 Å. A cylindrical projection[5] of this helix is shown in Fig. 2a; model building suggests that, of the three hydroxyl groups, two are involved in intramolecular hydrogen-bonding, and the third could be hydrogen bonded to a water molecule within the central cavity of the helix. The V_a-structure is converted by humidification first into a higher hydrate known as the V_h-form, which is thought[4] to have the same 6_1 helical conformation, but the helix separation is increased from 13.0 to 13.7 Å because of inclusion of water molecules between the chains. Further humidification, followed by soaking in water, leads to formation of the B-structure, with the A- and C-forms sometimes being observed as intermediates. The structure proposed for B-amylose[5] has chains having six residues per turn, repeating in 10.4 Å. It was further suggested[5] that the mechanism

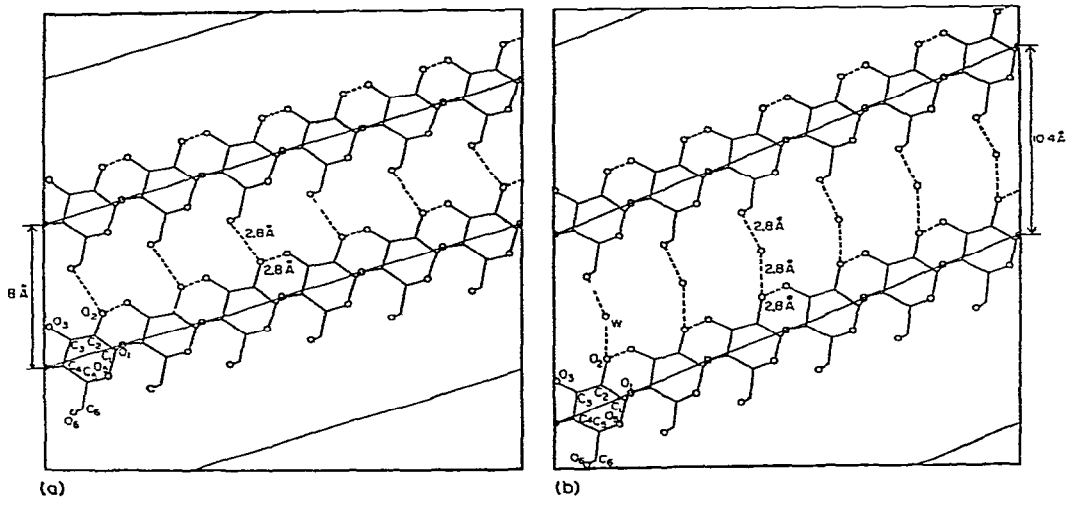

Fig. 2. (*a*) Cylindrical projection of the V-amylose helix. (*b*) Cylindrical projection of the proposed B-amylose helix, showing the inclusion of a water molecule, W, between successive turns. (Taken from Ref. 5, with permission of Academic Press).

for conversion from the V- into the B-form involves stretching out the helix, thereby breaking the inter-turn hydrogen bond, which is re-formed by insertion of a water molecule between the two hydroxyl groups, as shown in Fig. 2b. Other structures suggested for B-amylose are 3_1 and 4_1 single helices[6,7], and recently a double helix of 6_1 chains has been proposed[8]. The 3_1 and 4_1 chains are considered sterically unacceptable[5]. The double-helix structure appears incompatible with the ease of conversion from the V- to the B-form, but requires further study by calculation of the X-ray intensities.

During the last 20 years, considerable structural information has been obtained for other polysaccharides, such as cellulose, chitin, and xylan, from their infrared spectra. However, a number of difficulties are encountered when applying i.r. spectroscopy to starch polysaccharides. Most published work on polysaccharides has concentrated on interpretation of the O–H and C–H stretching regions which, unfortunately, are poorly resolved for the various forms of amylose, because of the water content of the specimens. The spectral differences between the polymorphic forms are observed mainly in the region below 1500 cm^{-1}. We have examined the Raman spectra of V_a-, V_h-, and B-amylose and have interpreted the observed differences, based on the band assignments in papers I and II of this series[9,10]. Additional information has been obtained by examination of the spectra of the cyclic oligomers: cyclohexa- and cycloheptaamylose. These observations have been correlated with the spectral data for amylose in aqueous and organic solvents, which have allowed conclusions to be drawn concerning the conformation in solution.

EXPERIMENTAL

All spectra were recorded with a laser Raman spectrometer constructed in this laboratory. The essential features of the instrument comprise a Spectra-Physics argon-ion laser having a maximum power of 1.5 W at both 488.0 and 514.5 nm, a Spex 1400 double monochromator, a Spex 1430 sample illuminator, and a photon-counting system. The light emitted from the laser is linearly polarized, perpendicular to the scattering plane, when incident on the sample. All spectra were recorded by using the 514.5-nm exciting line at a scan rate of 23 cm^{-1} per min; the time constant was 4 sec and the slit widths were adjusted between 100 and 160 μm. The wavelength accuracy ranged from ± 2 cm^{-1} for sharp or intense lines to ± 4 cm^{-1} for broad or weak lines.

Specimens of potato amylose (mol. wt. $\geq$ 150,000) were obtained from Pierce Chemical Company, and prepared initially as the butyl alcohol complex by precipitation as single crystals following the procedure of Manley[11]. A 0.5% solution of amylose in M sodium hydroxide was neutralized with HCl to pH 7.0 and then heated to 90–95°, whereupon an excess of hot butyl alcohol was added. After isothermal crystallization at 30°, the amylose–butyl alcohol complex was filtered off and washed three times with methanol. The complex was dried under vacuum for 24 h at 40°. The resulting amylose was the V_a-form. V_h-Amylose was prepared by exposing a specimen of V_a-amylose to 100% relative humidity for 24 h. B-Amylose specimens were

prepared by placing 2–3 drops of distilled, de-ionized water onto a V_a or V_h specimen, and allowing the specimen to stand for 24 h prior to spectral analysis. The use of distilled water without de-ionization caused the specimen to fluoresce in the laser beam, probably because of dissolved ions.

In order to investigate the effects of deuterium exchange in amylose, a specimen of the V_a-form was placed in a 1-mm glass capillary with D_2O, the amylose and D_2O being separated by glass wool (cotton was not used because it also undergoes deuterium exchange and has a spectrum similar to amylose). The capillary was sealed and the amylose allowed to equilibrate with D_2O for 48 h prior to analysis.

X-Ray diffraction scans were recorded for the solid-state specimens and the observed *d*-spacings compared with those reported for the V- and B-forms in order to confirm that the samples did indeed have the desired structure. The diffraction unit was a General Electric X-Ray diffractometer, model XRD-6.

Solutions of amylose were prepared in fully deuterated methyl sulfoxide (Me_2SO-d_6) and in aqueous (H_2O) 6M lithium bromide. The concentration of amylose was approximately 5% in both cases. The solutions were filtered through a Millipore "Solvinert" filter (0.5-μm pore size) in order to remove any dust particles and/or undissolved amylose.

Specimens of cyclohexa- and cycloheptaamylose were obtained from Sigma Chemical Company.

RESULTS AND DISCUSSION

1. The Raman spectra of V_a-, V_h-, and B-amylose. — The Raman spectra in the range 1500–300 cm^{-1} for V_a-, V_h-, and B-amylose are shown in Fig. 3a–c respectively, and Fig. 3d shows the spectrum of deuterated V_h-amylose. The frequencies of the lines observed in Figs. 3a–c and those for α-D-glucose[10] are listed in Table I. The Raman spectra recorded for crystalline cyclohexa- and cycloheptaamylose are shown in Fig. 4a–b.

Only small differences can be seen (Table I) between the data for amylose and α-D-glucose, with most of the observed lines occurring at approximately the same frequencies. In view of the relatively large size and cyclic structure of the glucose ring, it is expected that most of the vibrational modes observed in the amylose spectrum can be assigned to vibrations occurring in the individual residue, with only a few additional lines arising from coupling of modes between residues.

As can be seen in Fig. 3, the spectra of the three polymorphic forms of amylose are very similar. The differences between the data for the V_a- and V_h-forms appear negligible. If the only difference between the V_a and V_h crystal forms is the incorporation of water between amylose chains in the crystal lattice, then the effect of hydration on the V_h spectrum should be minimal, as the degree of inter-chain hydrogen bonding is thought to be small. If there existed a high degree of inter-chain hydrogen bonding in the V_a crystal lattice, there would be expected appreciable changes in the spectra following hydration of a V_a specimen.

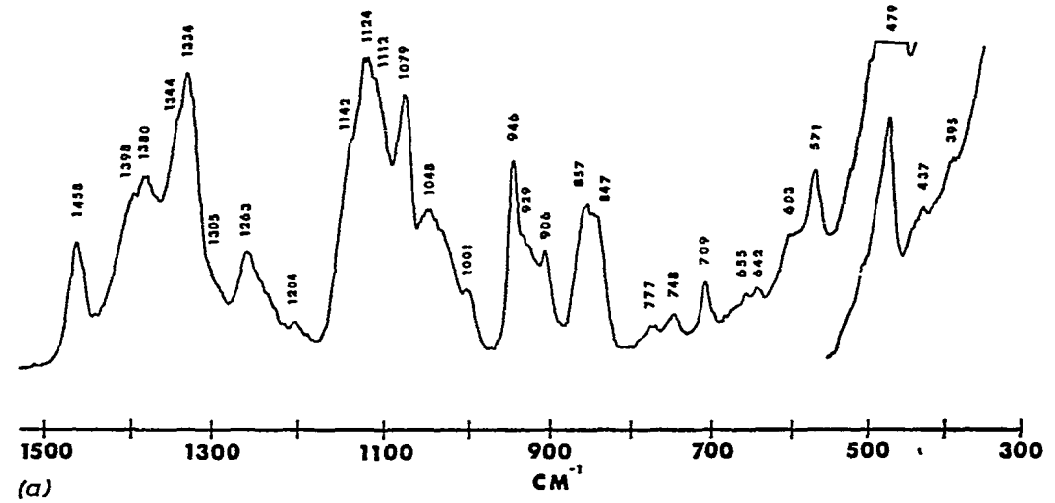
1458
1398
1380
1344
1336
1305
1263
1204
1142
1124
1112
1079
1048
1001
946
929
906
857
847
777
748
709
655
642
603
571
479
437
395
1500
1300
1100
900
700
500
300
(a)
CM-1

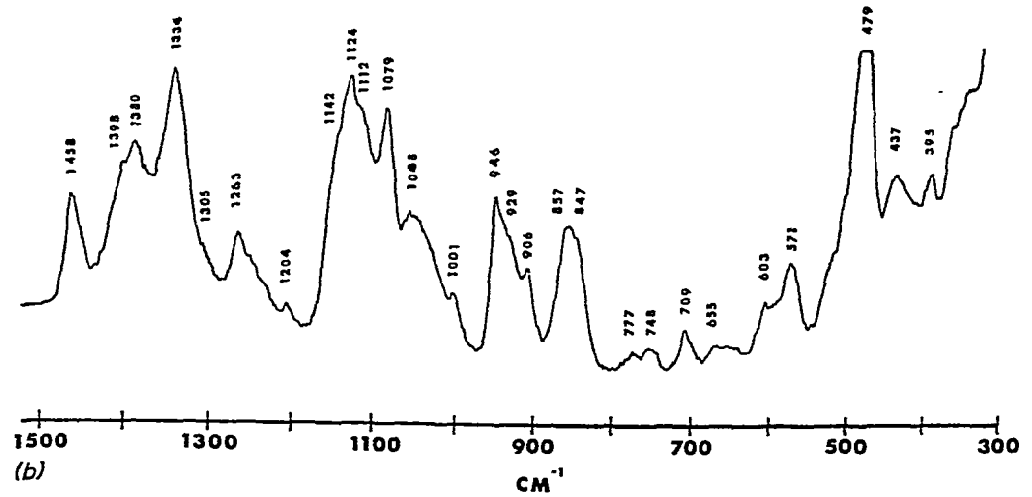
1458
1398
1380
1336
1305
1263
1204
1142
1124
1112
1079
1048
1001
946
929
906
857
847
777
748
709
655
603
571
479
437
395
1500
1300
1100
900
700
500
300
(b)
CM-1

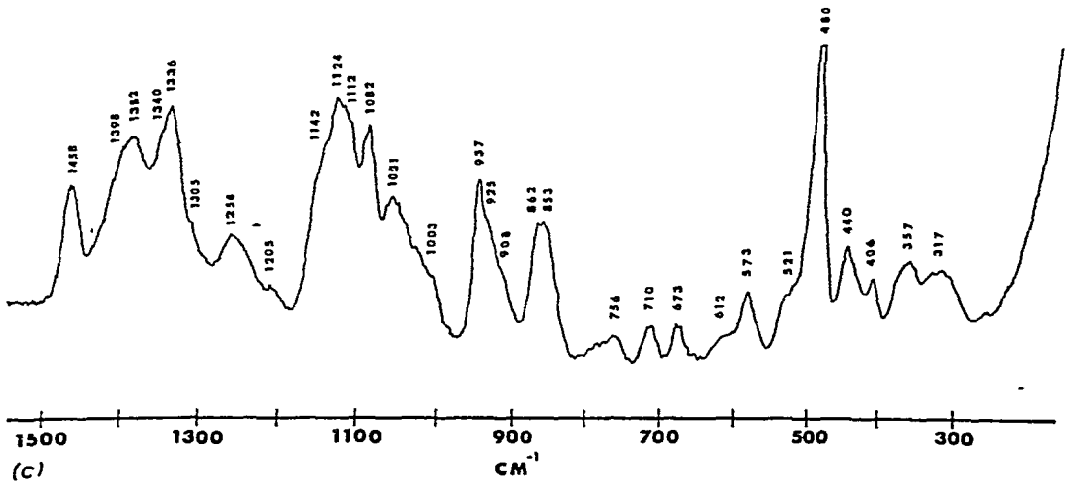
1458
1398
1382
1340
1336
1305
1256
1205
1142
1124
1112
1082
1021
1003
937
925
908
862
853
756
710
673
612
573
521
480
440
406
357
317
1500
1300
1100
900
700
500
300
(c)
CM-1

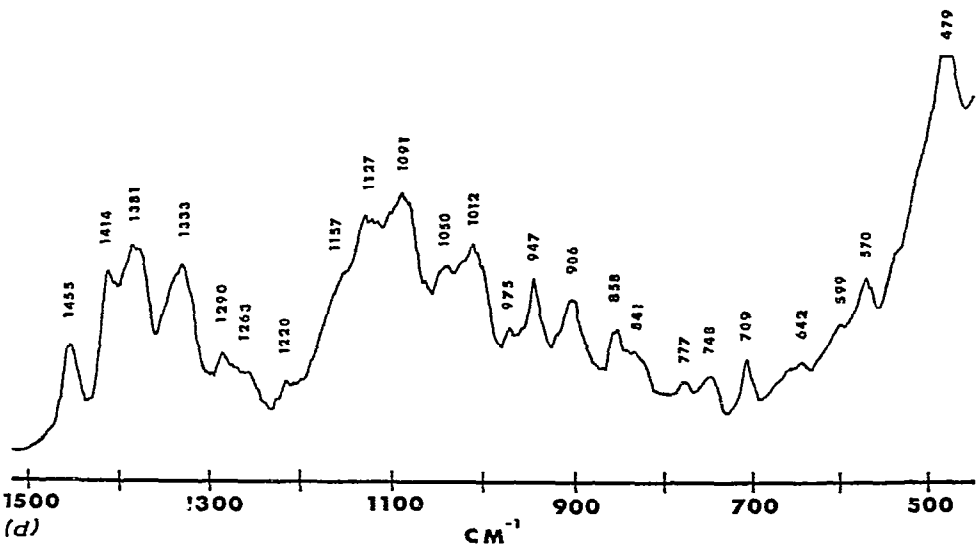

Fig. 3. The Raman spectra in the region 1500 to 300 cm^{-1} for crystalline specimens of (*a*) V_a-amylose, (*b*) V_h-amylose, (*c*) B-amylose, and (*d*) deuterated V_h-amylose.

2. Conversion of V- into B-amylose. — On conversion of V-amylose into the B-form, a number of changes occur in the spectrum. Lines at 1263 and 946 cm^{-1} appear to shift to the lower frequencies of 1254 and 936 cm^{-1}, respectively. In addition, significant decreases in intensity are detected for the lines at 2940 and 1334 cm^{-1}, relative to neighboring lines. These differences can be seen in Fig. 5, where the regions of the spectra containing these lines are compared.

On deuteration, the line at 1263 cm^{-1} decreases in intensity, (Fig. 3d), and a new line at 1290 cm^{-1} is observed. This effect parallels the changes on deuteration observed by Vasko *et al.*[9] for D-glucose, cellobiose, and maltose. These workers assigned the band in the 1260–1280 cm^{-1} region for the latter carbohydrates to a mode involving the CH_2OH side-chain, as no such deuteration effects were observed for dextran, which has α-D-(1→6) linkages. Thus, the line at 1263 cm^{-1} is probably due to a complex mode involving the CH_2OH side-chain in amylose. As such, the frequency variations observed for this mode during the V→B conversion are consistent with the proposed mechanism[5] for the change, which is believed to involve breaking the intra-chain hydrogen bonds.

A similar explanation can be made for the intensity changes observed for the 2940 and 1334 cm^{-1} lines. The former line is assigned to the CH_2 anti-symmetric stretching vibration, as it occurs close to the frequency of 2945 cm^{-1} for native cellulose[12,13]. The line at 1334 cm^{-1} is assigned as a CH_2-related deformation mode (probably the twisting mode). This mode occurs at 1335 cm^{-1} for α-D-glucose but is not observed for D-glucose-6,6-d_2 in which the CH_2 group is replaced by CD_2. The observed changes for these two lines are again consistent with a mechanism for the V→B conversion that involves changing of the bonding for the CH_2OH groups. A

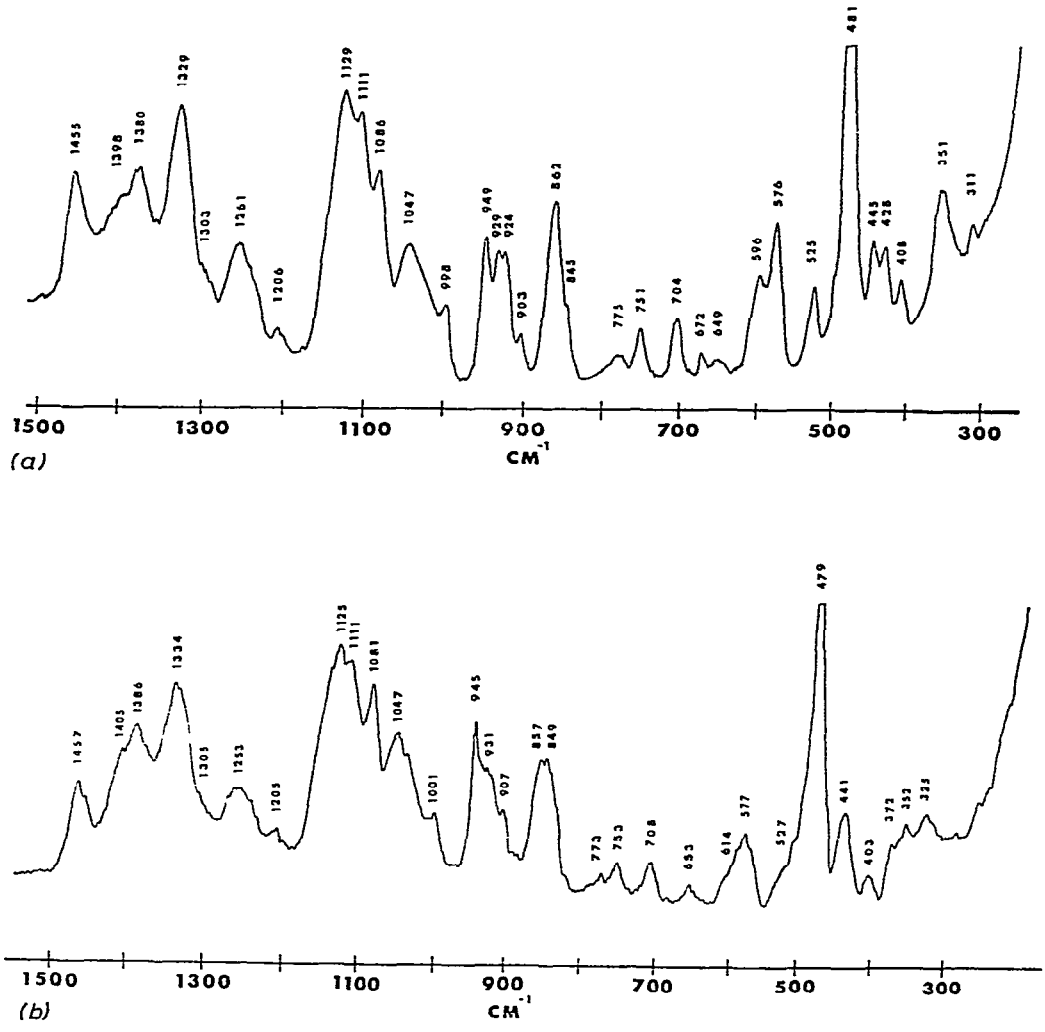

Fig. 4. The Raman spectra in the region 1500 to 300 cm^{-1} for crystalline specimens of (*a*) cyclohexaamylose and (*b*) cycloheptaamylose.

similar change of intensity occurs for cellulose on conversion from form I into form II: a significant decrease in intensity occurs in the band at 1430 cm^{-1}, assigned to the CH_2 symmetric bending-mode[14], which is probably due to changes in the hydrogen-bond network involving the CH_2OH groups.

The line at 946 cm^{-1} in the spectra of the V_a- and V_h-forms occurs at 936 cm^{-1} for B-amylose. No such line occurs for α-D-glucose, for which no scattering occurs between 914 and 998 cm^{-1}. This suggests that the line for amylose in the 940 cm^{-1} region is due to the α-D-(1→4) linkage. No such line occurs for maltose, the disaccharide analog of amylose, but a line is observed at 949 cm^{-1} for cyclohexa-

TABLE I

VIBRATIONAL ASSIGNMENTS FOR V_a, V_h, B-AMYLOSE, AND α-D-GLUCOSE

Frequency (cm^{-1})				
V_a-Amylose	*V_h-Amylose*	*B-Amylose*	*α-D-Glucose*	*Assignment*
1458 m[a]	1458 m	1458 m	1462	CH_2 (deformation)
			1433	
1398 m(sh)	1398 m(sh)	1398 m(sh)	1408	C–H bending
1380 m	1380 m	1382 m	1375	
1344 w(sh)		1340 w(sh)	1346	C–O–H bending
1334 s	1334 s	1336 s	1335	CH_2 (deformation) and C–O–H bending
1305 w(sh)	1305 w(sh)	1305 w(sh)	1298	C–H bending
1263 m	1263 m	1254 m	1272	CH_2OH related mode
			1224	CH_2 (deformation)
1204 w	1204 w	1205 w	1206	
1142 m(sh)	1142 m(sh)	1142 m(sh)	1153	C–O, C–C, C–H related modes
1124 s	1124 s	1124 s	1124	
1112 m(sh)	1112 m(sh)	1112 m(sh)	1115	
1079 s	1079 s	1082 s	1076	C–O–H bending
1048 m	1048 m	1051 m	1054	
			1022	C–O–H bending
1001 m(sh)	1001 m(sh)	1003 w(sh)	998	CH_2 (related mode)
946 m	946 m	936 m		skeletal mode involving α-(1→4) linkage
929 w(sh)	929 w(sh)	925 w(sh)	914	C–O–H bending
906 m(sh)	906 m(sh)	908 w(sh)	897	
857 m	857 m	862 m	859	
847 m(sh)	847 m(sh)	853 m	840	C–1–H bending (α-configuration)
777 w	777 w		779	
748 w	748 w	756 w	748	C–C, C–C stretchings
709 w	709 w	710 w	704	
		673 w		
655 w	655 w			
642 w	642 w		648	
603 w(sh)	603 w(sh)	612 w(sh)	601	
571 m	571 m	573 m	581	
			554	
		521 m(sh)	522	
479 vs	479 vs	480 vs	495	skeletal modes
437 w	437 w	440 w	441	
			425	
395 w	395 w	406 w	405	
			397	
		357 w	364	
		317 w	303	

[a]Key to intensities: vs, very strong; m, moderate; w, weak; sh, shoulder.

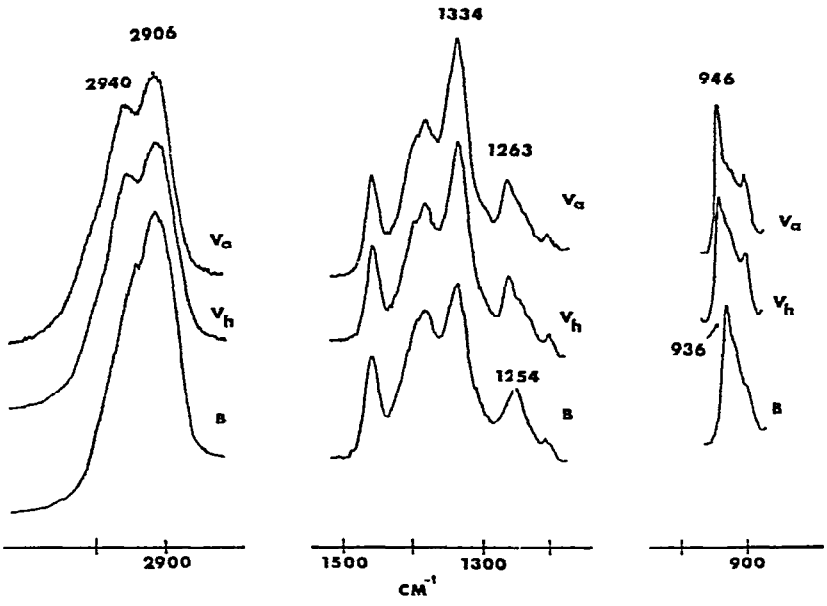

Fig. 5. Superimposed regions of the spectra of V_a-, V_h-, and B-amylose, showing changes during the V→B conversion.

amylose and at 945 cm^{-1} for cycloheptaamylose, (Fig. 4). Vasko *et al.*[10] have shown that the vibrational modes for α-D-glucose are highly coupled, and it is probable that the line for amylose at ~940 cm^{-1} is a coupled mode involving cooperative vibrations of the glycosidic oxygen atom and the ring atoms. Chain length may be crucial for this coupling, which may account for the non-appearance of this mode for maltose. We conclude that this line in the 940 cm^{-1} region is a skeletal mode involving the α-D-(1→4) linkage. Casu and Reggiani[15] attributed the i.r. band at 948 cm^{-1} for cyclohexaamylose to a ring vibration, and considered that it shifted to 928 cm^{-1} in amylose, which showed no band at ~940 cm^{-1} in the i.r. However, our Raman data show lines at 946 and 929 cm^{-1} for both V-amylose and cyclohexaamylose. Furthermore, if the band at ~940 cm^{-1} is caused by a ring mode, it should be seen for α-D-glucose and maltose.

The change in frequency for the line at ~940 cm^{-1} can be correlated with the extension of the helix. Cyclohexaamylose, V-, and B-amylose, all having six-fold symmetry, have a rise per residue of zero, 1.33 and 1.73 Å, respectively, and the skeletal mode is at 949, 946, and 936 cm^{-1}, in turn. The three structures differ in the dihedral angles, that is, the rotations of successive residues with respect to the glycosidic bonds. Furthermore, the C-1–O-1–C-4′ glycosidic bond-angle[16] in cyclohexaamylose is 119.1°, which represents a slight strain with respect to the optimum value of 117°. This strain can be progressively relieved in the V and B helices, and in cycloheptaamylose where the skeletal mode is at 945 cm^{-1}. The frequency changes observed are consistent with changes in rotation angles, and relief of strain, and in

accord with the conversion of V- into B-amylose by extension of the 6_1 helix. It is stressed, however, that all that can be said is that the differences between the spectra of the two forms are *consistent* with the proposed mechanism[5] for V→B conversion. At this stage it is not possible to rule out other conformations for the B-form, which may well have different CH_2 and linkage motions. Further work is now in progress on oriented specimens in order to resolve questions of the conformation from the dichroism data.

3. Deuteration of V-amylose. — The Raman spectrum of V_h-amylose in equilibrium with D_2O vapor is shown in Fig. 3d. On comparison with the spectrum of the non-deuterated specimen (Fig. 3b), decreases in intensity are observed for lines at 1334, 1263, 1079, and 929 cm^{-1}. These lines have been assigned (Table I) to modes involving bending motions of the C–O–H groups. The lines at 1334 and 1263 cm^{-1} do not disappear completely, and the residual intensity is probably due to other overlapped modes or incomplete deuteration of the amylose specimen. Likewise, the lines at 1079 and 929 cm^{-1}, although no longer observed, may possibly be obscured by adjacent lines; nevertheless, intensity changes for these lines are observed and are reproducible. As discussed previously, the line at 1335 cm^{-1} for α-D-glucose has been shown to have a considerable CH_2 contribution, and it is likely that this mode for amylose has both CH_2 and C–O–H character. Further evidence that this is a coupled mode comes from the appearance, with deuteration, of a new line at a higher frequency (at 1414 cm^{-1}) which is probably a new mode resulting from decoupling of the CH_2 and C–O–H motions. New lines appear on deuteration at 1290, 1220, 1091, and 1012 cm^{-1}, and these are assigned as C–O–D related modes.

The assignments for the observed lines in the amylose spectra are given in Table I, based on the results in this paper and on comparison with the data for D-glucose, maltose, cellobiose, and dextran[9,10].

4. Raman spectra of amylose in solution. — To date, the conformation of amylose in aqueous and organic solvents has been a matter of controversy. A number of studies have been made of this problem by using viscosity, light scattering, and sedimentation techniques. The results of Banks and Greenwood [17–20] indicated that amylose in aqueous salt solutions exists as flexible, only moderately restricted chains, and the conformation was assumed to be a random coil. Other authors[21,22] support the view that amylose has a stiff, helical conformation in solution. A further model for the conformation in solution is the "interrupted helix", in which long helical segments, of about 120 D-glucose residues, alternate with short random-coil regions[23,24].

The Raman spectra of solutions of amylose in 6M aqueous lithium bromide and Me_2SO-d_6 are shown in Fig. 6a–b. In the case of the salt solution, the spectrum shows features similar to that for the solid B-amylose specimen; identifying lines are observed at 1255 and 938 cm^{-1}. In view of the sloping background it is difficult to be specific about the relative intensity of the line at 1336 cm^{-1}, but the intensity is less than that observed for the solid V-amylose. These results indicate, not surprisingly, that amylose does not have the V-conformation in aqueous salt solution. At present,

however, it is not possible to say whether or not the molecules form the B-helix in solution as the spectral characteristics for random amylose chains are not known.

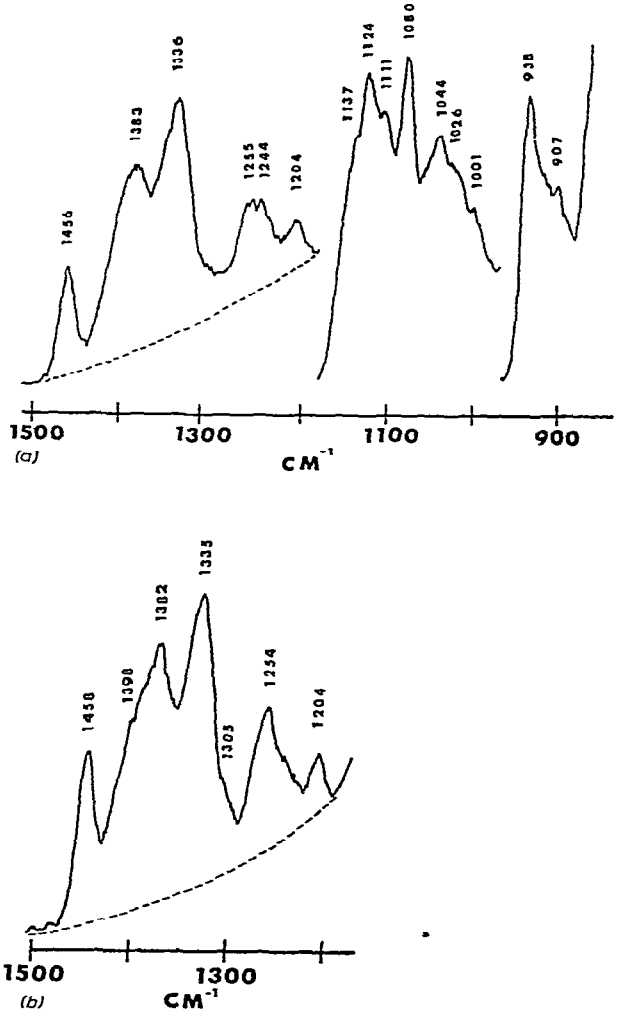

Fig. 6. (*a*) Raman spectrum of amylose in 6N lithium bromide solution (1500–800 cm^{-1} region); (*b*) Raman spectrum of amylose in Me_2SO-d_6 (1500–1200 cm^{-1} region). Dashed lines indicate the approximate base-lines resulting from scattering by the solvent.

The spectrum of amylose in Me_2SO-d_6 can only be recorded above 1200 cm^{-1}; below this figure intense scattering by the solvent occurs. A line is observed at 1254 cm^{-1}, which matches the data for B-amylose. Similarly, the relative intensity of the line at 1334 cm^{-1} is close to that observed for the B-form. These results are surprising, as crystallization of amylose from Me_2SO solution yields a V-structure. Our data indicate that amylose does not have the V-conformation in Me_2SO solution,

and the chains are probably extended, with the CH_2OH groups hydrogen-bonded to solvent molecules rather than involved in intramolecular linkages. These results are in agreement with the proton magnetic resonance studies of Casu *et al.*[25], who showed that whereas the 2-OH and 3'-OH groups spend sometime intramolecularly hydrogen-bonded, the CH_2OH hydroxyl groups are bonded to Me_2SO molecules. Further investigations of the conformation of amylose in solution are in progress.

ACKNOWLEDGMENT

This work was supported by NSF grant no. GB 32405.

REFERENCES

1 J. R. KATZ AND T. B. VAN ITALLIE, *Z. Physik. Chem.*, A150 (1930) 90.
2 R. BEAR AND D. FRENCH, *J. Amer. Chem. Soc.*, 63 (1941) 2298.
3 R. E. RUNDLE AND D. FRENCH, *J. Amer. Chem. Soc.*, 65 (1943) 558.
4 H. F. ZOBEL, A. D. FRENCH, AND M. E. HINKLE, *Biopolymers*, 5 (1967) 837.
5 J. BLACKWELL, A. SARKO, AND R. H. MARCHESSAULT, *J. Mol. Biol.*, 42 (1969) 379.
6 D. R. KREGER, *Biochim. Biophys. Acta*, 6 (1951) 406.
7 P. R. SUNDARARAJAN AND V. S. R. RAO, *Biopolymers*, 8 (1969) 313.
8 K. KAINUMA AND D. FRENCH, *Biopolymers*, 11 (1972) 2241.
9 P. D. VASKO, J. BLACKWELL, AND J. L. KOENIG, *Carbohyd. Res.*, 19 (1971) 297.
10 P. D. VASKO, J. BLACKWELL, AND J. L. KOENIG, *Carbohyd. Res.*, 23 (1972) 407.
11 R. ST. J. MANLEY, *J. Polymer Sci.*, A2 (1964) 4503.
12 R. H. MARCHESSAULT AND C. Y. LIANG, *J. Polymer Sci*, 43 (1960) 71.
13 J. BLACKWELL, P. D. VASKO, AND J. L. KOENIG, *J. Appl. Physics*, 41 (1970) 4375.
14 A. W. MCKENZIE AND H. G. HIGGINS, *Svensk Papperstidn*, 61 (1958) 893.
15 B. CASU AND M. REGGIANI, *J. Polymer Sci.*, C7 (1964) 171.
16 A. HYBL, R. E. RUNDLE, AND D. E. WILLIAMS, *J. Amer. Chem. Soc.*, 87 (1965) 2779.
17 W. BANKS AND C. T. GREENWOOD, *Eur. Polymer J.*, 5 (1969) 649.
18 W. BANKS, C. T. GREENWOOD, D. J. HOURSTON, AND A. R. PROCTER, *Polymer*, 12 (1971) 452.
19 W. BANKS AND C. T. GREENWOOD, *Biopolymers*, 11 (1972) 315.
20 W. BANKS AND C. T. GREENWOOD, *Biopolymers*, 12 (1971) 141.
21 V. S. R. RAO AND J. F. FOSTER, *Biopolymers*, 1 (1963) 527.
22 J. HOLLÓ AND J. SZEJTLI, *Staerke*, 10 (1958) 49.
23 J. SZEJTLI AND S. AUGUSTAT, *Staerke*, 19 (1967) 139.
24 S. R. ERLANDER AND H. L. GRIFFIN, *Staerke*, 19 (1967) 139.
25 B. CASU, M. REGGIANI, G. G. GALLO, AND A. VIGEVANI, *Tetrahedron*, 22 (1966) 3061.